Electronic Supplementary Material (ESI) for Biomaterials Science.

Supporting Information

Sustainable Glycerol Terpolycarbonates As Temporary Bioadhesives

Anjeza Petersen,[1§] Ngoc-Quynh Chu,[2§] Danielle M. Fitzgerald,[1] Ethan Z. McCaslin,[1] William A. Blessing,[2] Aaron H. Colby,[1] Yolonda L. Colson,[2*] and Mark W. Grinstaff [1*]

[1]Departments of Chemistry, Biomedical Engineering, and Medicine, Boston University, Boston, MA, 02215, USA.

[2]Divison of Thoracic Surgery, Massachusetts General Hospital, Harvard Medical School, Boston, MA, 02114, USA.

*Corresponding Authors: Mark W. Grinstaff mgin@bu.edu and Yolonda L. Colson ycolson@mgh.harvard.edu

Table of Contents

METHODS

General Information

All manipulations involving air- and/or water-sensitive compounds were carried out in a glovebox. All oxiranyl monomers were refluxed over CaH_2, and fractionally distilled under a nitrogen atmosphere prior to use. Carbon dioxide (99.995%, bone dry) was purchased from Airgas and used as received. Reagents were purchased from Sigma Aldrich and used as received. All measurements were taken from distinct samples. To artificially mimic high humidity conditions, a damp sponge was placed over the reaction vessel for 20 seconds prior to the polymerization.

NMR experiments

^{1}H and ^{13}C NMR spectra were recorded on a Varian 500 MHz type (^{1}H, 500MHz; ^{13}C, 125 MHz) spectrometer. Their peak frequencies were referenced against the solvent, chloroform-d at δ 7.24 for ^{1}H NMR and δ 77.23 ppm for ^{13}C NMR, respectively.

Gel Permeation Chromatography

All polymer molecular weights were determined by gel permeation chromatography versus polystyrene standards (Agilent Technologies) using THF as the eluent at a flow rate of 1.0 mL/min through a Styragel column (HR4E THF, 7.8 x 300 mm) with a Waters 2414 refractive index detector. For the polymer degradation studies, polymer molecular weights were determined versus polyethylene glycol standards (Agilent Technologies) using aqueous nitrite buffer as the eluent at a flow rate of 1.0 mL/min through an Aquagel-OH column (300 mm, 8 μm particle size) with a Waters 2414 regractive index detector.

MALDI-ToF

MALDI-ToF mass values for polymers were determined using a Bruker autoflex Speed MALDI-ToF mass spectrometer equipped with a SMART-beam II and a flash detector. Samples were prepared by dissolving in a 1:1 vol/vol mixture of matrix solvent (10 mg/mL solution of dithranol in THF with 0.1% AgTFA) and 10 mg polymer dissolved in minimal amount THF.

Differential Scanning Calorimetry

The thermal properties of the polymers were measured by Differential Scanning Calorimetry (DSC) using a TA Q 100) under a nitrogen atmosphere (nitrogen flow rate: 60 mL min^{-1}). All samples were tested at a heating rate of 10 °C/min and a cooling rate of 10 °C/min from -40 to 80 °C. The weight of all samples was between 2 to 10 mg and the samples underwent three heat-cool-heat cycles. The glass transition temperature, Tg, was noted in the DSC-thermogram as the midpoint temperature of the glass transition peak in the second heating cycle (Supplementary Fig. 9).

180^o Peel Strength

The peel adhesion test was carried out at room temperature (22°C) by using Fischerbrand glass microscope (SiO_2) slides (base stock) and a A4 paper (face stock) as substrates.

The face dimensions for the glass slides were 7.6 cm × 2.6 cm. The adhesive was coated on the non-frosted surface of the glass plate containing a coating area of 2 cm × 2.6 cm with a coating thickness of ~30 µm. Then, the paper substrate was stuck on the coated glass slide with moderate human finger pressure. The sample was let to settle for 1 minute prior to testing on an Intron 5944 with peel speed operating at 360 mm/min.

Commercial all-purpose Duct Tape® (3M 2929) and Scotch Tape® (3m 810) were used as received, (besides width modifications) and stuck to the glass. Duct tape was cut to 2.6 cm of width, scotch tape was not modified. Three separate specimens were used for each adhesive formulation in this test. The average peak from the load propagation graph was used to calculate the peeling force. Peel strength is defined as the average load per width of the bondline required to separate progressively a flexible member from a rigid member (ASTM D 903).

Additionally, the Duct Tape® adhesive was dissolved from its commercial backing using dichloromethane and dried under reduced pressure. Peel testing for this adhesive was completed as described above using A4 paper as the face stock (n=3). Duct Tape® was also analyzed as

received, to act as a control (n=3) (see Figure S12). Adhesive values were normalized to the average of the control results and analysis of these sample results through a two-tailed, unpaired t test yields a p value of 0.71 which is not statistically significant (α = 0.05). This indicates that the strength of adhesives using A4 paper face stocks are comparable to commercial products and are appropriate for use in this manuscript.

Probe Tack

All tack testing were performed on a Discovery Hybrid Rheometer (DHR-2 series) with 8 mm stainless steel-sand blasted parallel plate geometry with a Peltier plate. The adhesive was placed on the bottom plate and a top probe moving at 100 m/sec rested on the adhesive until the desired axial force was reached. After 5 seconds, the top probe pulled away at a rate of 100 m/sec.The peak of the force curve is defined as the tack strength (T_s) and the area under the curve is defined as the tack energy (T_e) as calculated by eq. (1), where A denotes the surface area (m^2) of the probe, r is the rate of probe separation in debonding (m/s), F is the force (N) measured during debonding, and t is the time in seconds;

$$T_e = 2\,x\left[\frac{r}{A}\int_{ti}^{tf} F(t)dt\right] \qquad (1)$$

Frequency Sweeps

All oscillatory sweeps were performed on a Discovery Hybrid Rheometer (DHR-2 series) with 8 mm stainless steel parallel plate geometry with a gap size of 50 μm. Frequency sweeps were performed from 0.1 to 100 rad/s or 1 to 500 rad/s at 1% strain (determined to be in the linear viscoelastic region with a previous strain sweep) at specified temperatures (20 °C, 25 °C, 37 °C, 50 °C) controlled by a Peltier plate.

Cell Culture

NIH 3T3 murine fibroblasts (ATCC) were cultured in Dulbecco's modified Eagle's medium supplemented with 10% bovine calf serum and 1% penicillin-streptomycin. RAW 264.7 murine macrophages were cultured in Dulbecco's modified Eagle's medium supplemented with 10%

fetal bovine serum and 1% penicillin-streptomycin. Cells were maintained in a sterile, humidified environment at 37 °C with 5% CO_2.

In Vitro Evaluation of Cytotoxicity

NIH 3T3 cells were seeded in a 96-well plate at a density of 20,000 cells/well and were allowed to adhere for 24 h. The media was then replaced with fresh media, and cells were incubated with polymer samples in 5% DMSO using transwell inserts (0.4 μm pores). Cell viability was assessed 24 h after treatment via the MTS in vitro cytotoxicity assay (CellTiter 96 Aqueous One, Promega) and compared to the media only control. The average of two experiments (N=2) in which n=6 per polymer concentration.

In Vitro Evaluation of Immunogenicity

RAW 264.7 cells were seeded in a 96-well plate at a density of 30,000 cells/well and were allowed to adhere for 24 h. The media was then replaced with fresh media, and cells were incubated with polymer samples in 5% DMSO using transwell inserts (0.4 μm pores). IL-6 levels were measured via ELISA kit (Abcam) and compared to those of RAW 264.7 treated with lipopolysaccharide—a molecule known to stimulate IL-6 production and immunogenicity *in vitro* (n=6).

Ex Vivo Evaluation of Performance

The collagen buttress (bovine pericardium, PERI-STRIP DRY®, Synovis) was coated without the aid of solvents or heat (SI Figure S11A; Movie 1). Specifically, we applied neat (GA-*co*-GB)-87 to a metal spatula and used the spatula to spread the adhesive onto the collagen buttress. A thin layer of adhesice was applied, approximately 0.5 mm in thickness. The adhesive coated buttress was then used. As shown in SI Figure S11B (movie 2), the stapler jaws (ENDO GIA™ Ultra universal 12mm stapler and ENDO GIA™ 45mm articulating tri-staple reload, Medtronic) bind to and release the buttress from the packaging after application of a mild force on jaw closure. Motions of sequential jaw closing/opening and rotation did not detach the buttress from the device (SI Figure S11C; Movie 3). After the stapler is fired, the staples secure the buttress to the tissues

allowing separation of the buttress from the jaws of the stapler simply by opening the stapler (SI Figure S11D; Movie 4). To demonstrate clinical application, we used the device to resect a small section of sheep lung *ex vivo*, akin to wedge resections of human lung parenchyma performed for lung cancer or biopsy of lung pathology. As is done clinically, the staple line was tested for an air leak by submerging the staple line under water and sequentially inflating and deflating the lung with air under positive pressure for 5 "breaths" (25 cm of water). We observed no air leaks (absence of bubbles) indicating that the staple line within the lung parenchyma was properly sealed.

SYNTHETIC PROCEDURES

Synthesis of Epoxide Monomers

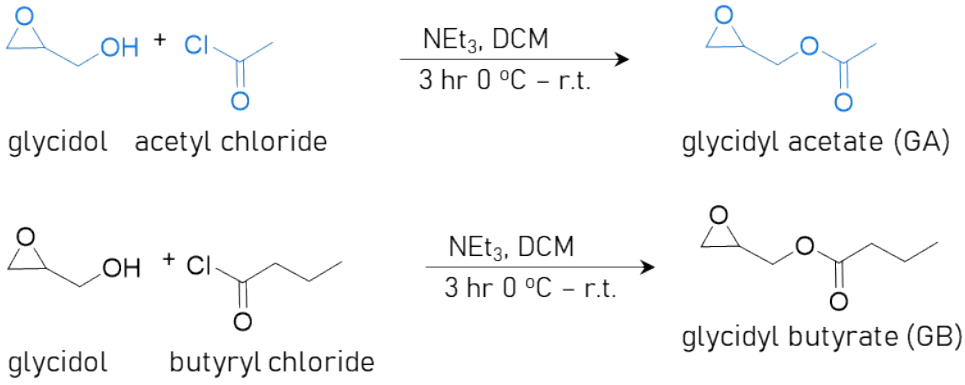

Scheme S1. Synthesis of glycidyl acetate and glycidyl butyrate.

Glycidyl acetate/glycidyl butyrate was synthesized according to previous literature.[1] A roundbottom flask was charged with 300 ml dichloromethane, trimethylamine (84 mL, 600 mmol) and glycidol (20 mL, 300 mmol). The reaction was placed in an icebath and stirred for 30 minutes. Acetyl Chloride (23.4 mL, 333 mmol) /butyryl chloride (35 mL, 333 mmol) was added dropwise and the reaction was stirred for another 3 hours at room temperature. The subsequent solution was filtered to remove the salt precipitate. The organic layer was washed with saturated

sodium bicarbonate (300 mL) three times, once with brine (300 mL), dried over sodium sulfate, and evaporated off under low pressure. The crude yellow product was fraction distilled under vacuum at 80°C/110 °C to produce pure glycidyl acetate/glycidyl butyrate as a clear oil. (29 mL, 272 mmol, 91% yield)/(33 mL, 229 mmol, 76% yield).

Synthesis of Catalyst

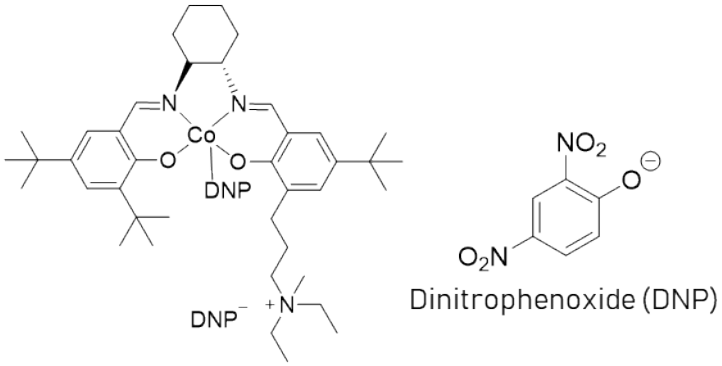

Scheme S2. Structure of (S,S)-[SalcyCo^{III}DNP]DNP.

The salen ligand cobalt catalyst was synthesized as previously described by Lu *et al.*[2,3]

Representative Polymer Synthesis

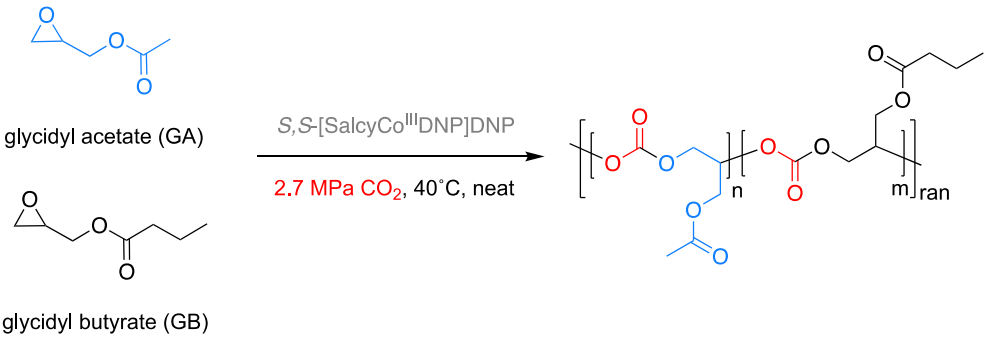

Scheme S3. Synthesis of polycarbonate terpolymers.

In a glovebox, glycidyl butyrate (0.67 mL, 5 mmol) glycidyl acetate (0.51 mL, 5 mmol) were added into a high pressure autoclave, followed by the addition of *(S,S)*-SalcyCo^{III}DNP (5.21 mg, 0.005 mmol). The autoclave was transferred out of the glovebox and charged with CO_2 to 2.7 MPa. The reaction was allowed to run at 40 °C for 10 hr. Subsequently, the reaction vessel was placed in an ice bath for 10 minutes and the CO_2 pressure was released. The reaction mixture was diluted in minimal amount DCM. The mixture was added dropwise into cold MeOH (50 ml) and the precipitated polymer was collected. The precipitation was repeated for a total of 3 times until complete removal of the catalyst and unreacted monomer. The resultant material was dried under vacuum to yield ~ 300 mg of a viscous liquid/brittle solid.

FIGURES

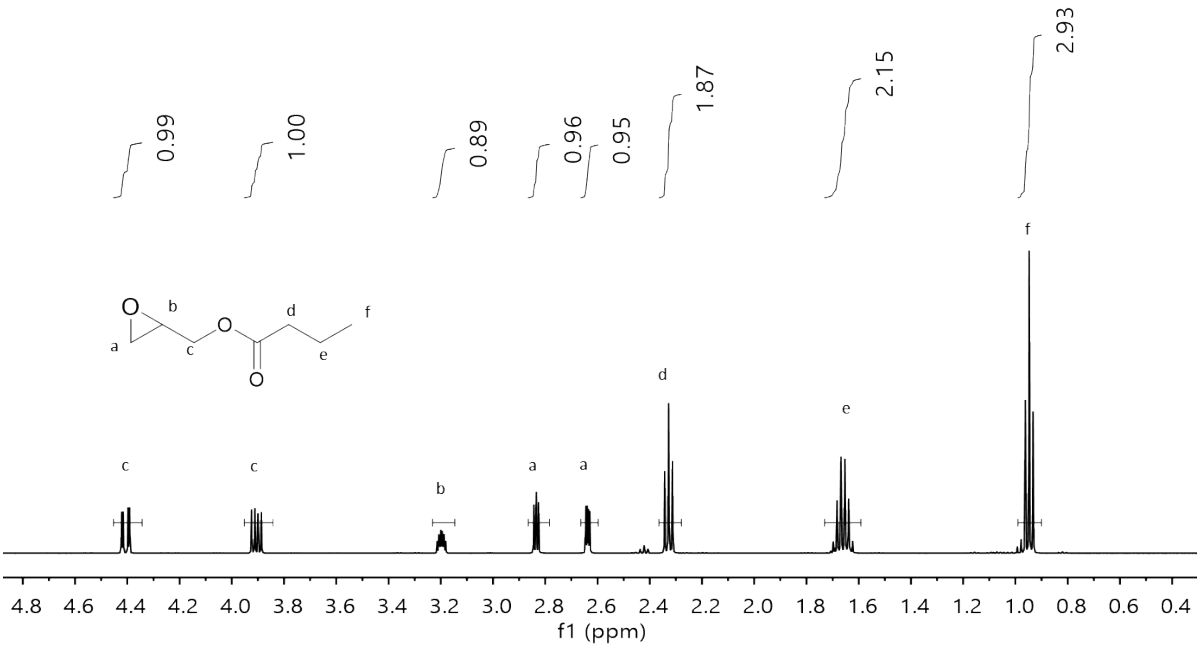

Figure S1. 1H NMR spectrum of glycidyl butyrate in $CDCl_3$.

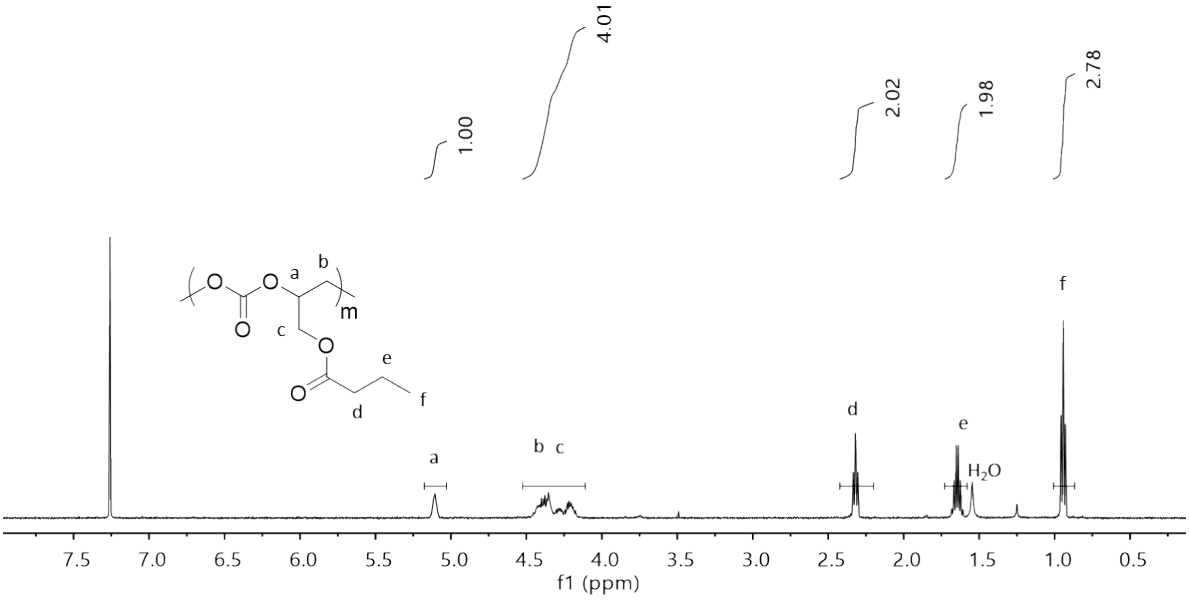

Figure S2. ^{1}H NMR spectrum of poly(glycidyl butyrate carbonate) in $CDCl_3$.

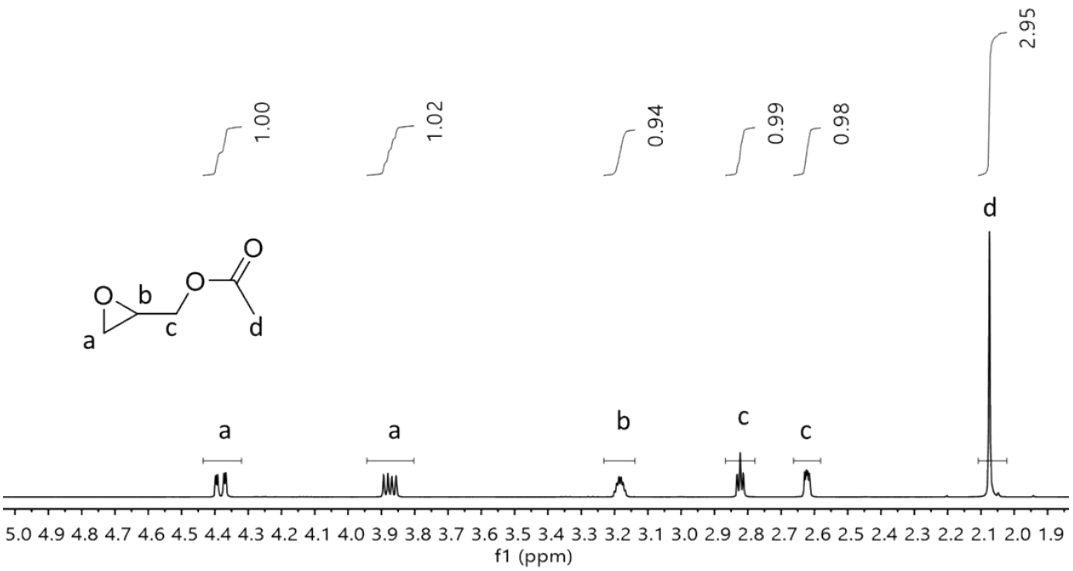

Figure S3. ^{11}H NMR spectrum of glycidyl acetate in $CDCl_3$.

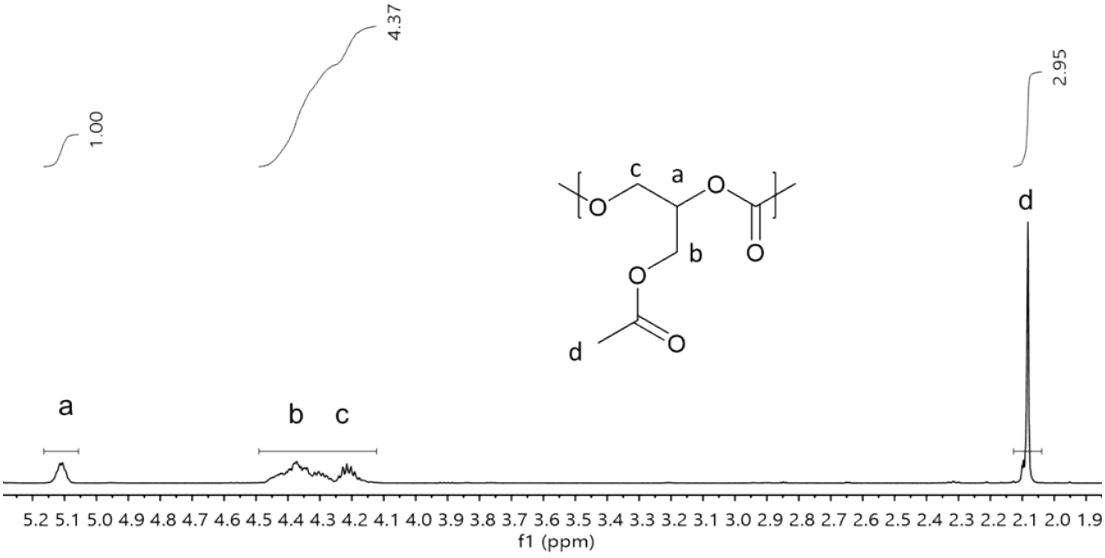

Figure S4. ^{1}H NMR spectrum of poly(glycidyl acetate carbonate) in $CDCl_3$.

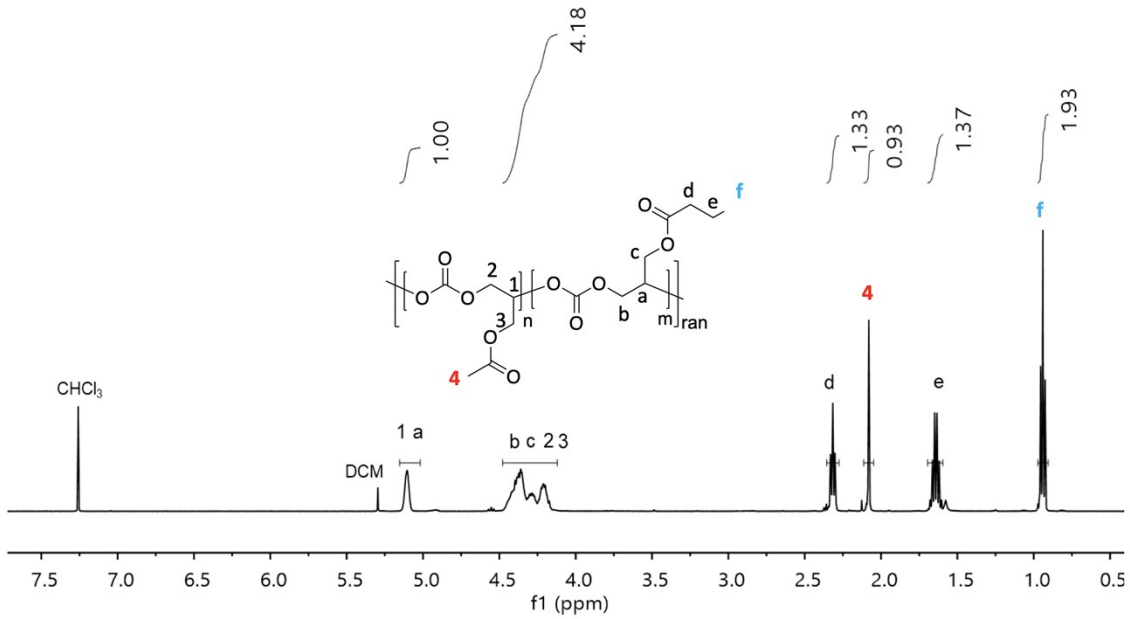

Figure S5. ^{1}H NMR spectrum of poly(GA-co-GB carbonate) in $CDCl_3$.

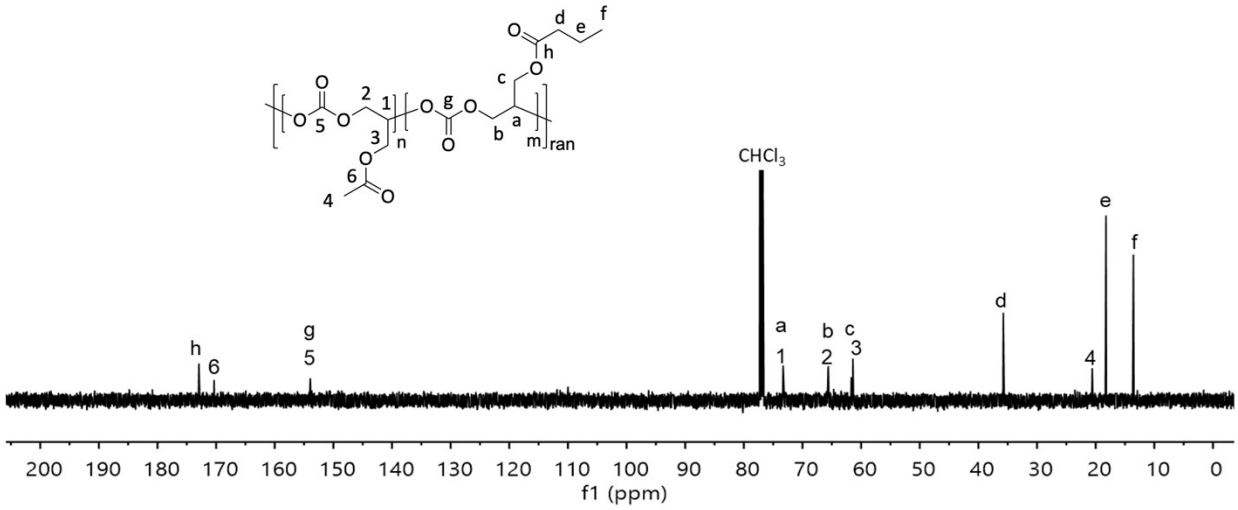

Figure S6. ^{13}C NMR spectrum of poly(GA-co-GB carbonate) in $CDCl_3$.

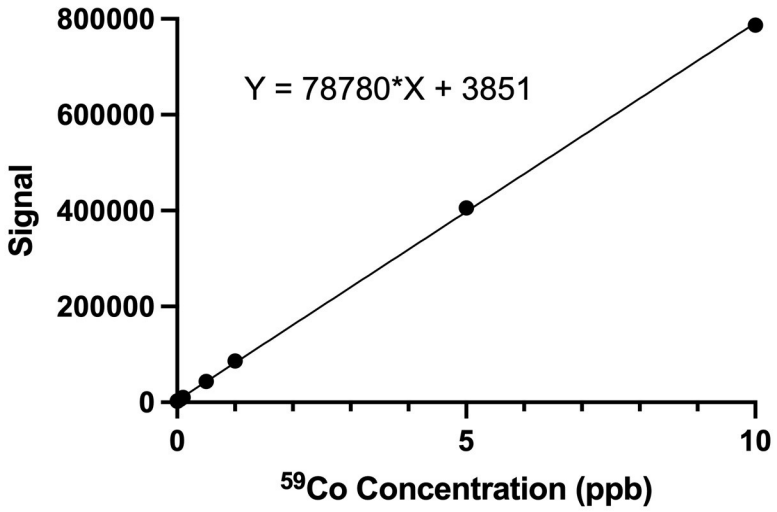

Figure S7. ICP-MS calibration curve for ^{59}Co from 0.001 to 10 ppb. R^2 = 0.9998. LOD signal = 2026.771.

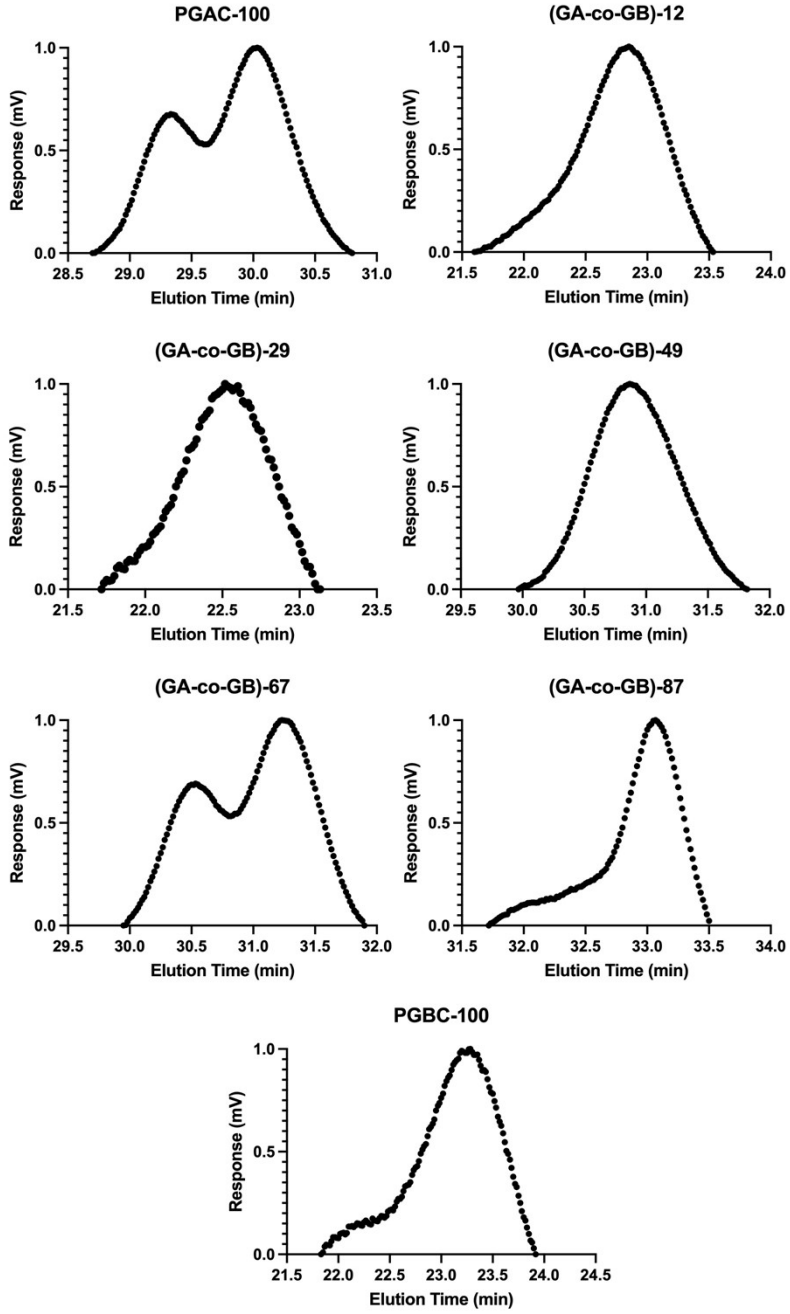

Figure S8. GPC trace of poly(glycerol carbonate) derivatives. Polymers demonstrating bimodal distirbutions are due to the presence of adventitious water. Response was normalized to the highest value in each GPC trace.

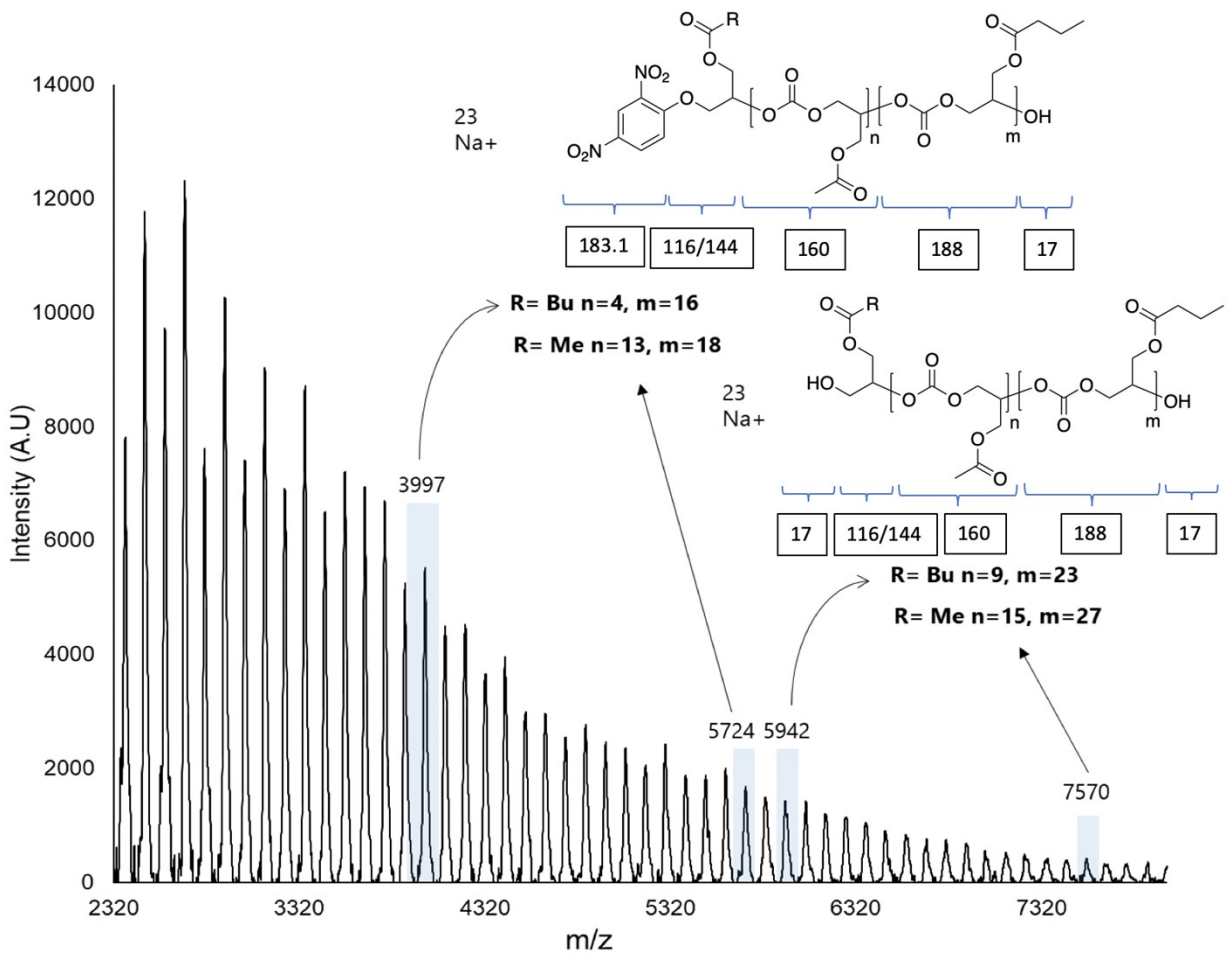

Figure S9. MALDI-TOF spectrum of (GA-co-GB)-67.

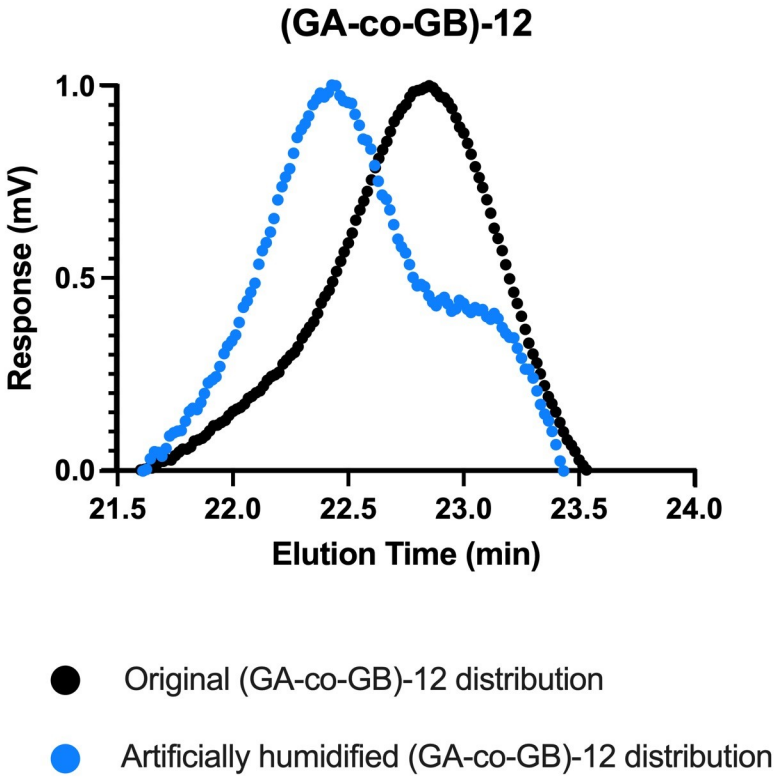

Figure S10. GPC trace of (GA-*co*-GB)-12 overlayed with GPC trace of (GA-*co*-GB)-12 polymerized in an artificially humidified environment. Response was normalized to the highest value in each GPC trace.

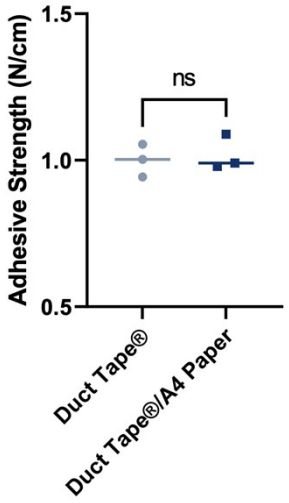

Figure S11. Comparison of the adhesive strength of Duct Tape® (control) to Duct Tape® adhesive with A4 paper as the face stock (adhesive extracted from commercial backing and applied to A4 paper). Adhesive strength values are normalized to the average of the control samples. The difference between Duct Tape® and Duct Tape®/A4 Paper is not significant ($p > 0.05$).

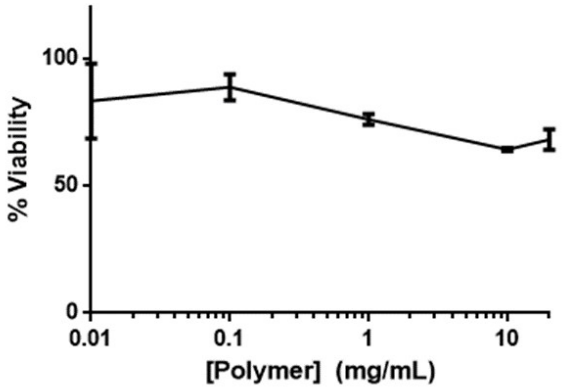

Figure S12. Cytotoxicity of GA-co-GB-87 to NIH 3T3 fibroblasts as a function of concentration. At the higher dose minimal toxicity observed.

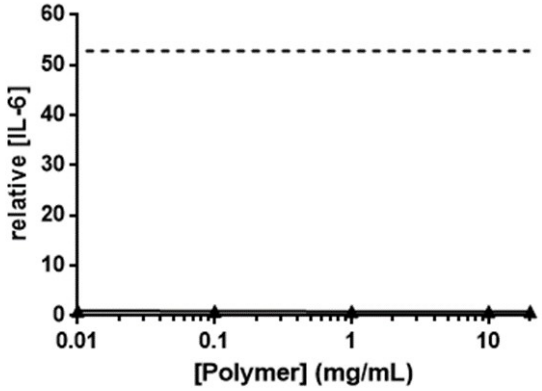

Figure S13. Immunogenicity of GA-co-GB-87 to RAW 264.7 macrophages at various concentrations. IL-6 is not upregulated at any concentration of polymer and shows no *in vitro* immunogenicity. The dashed line represents relative expression of IL-6 with lipopolysaccharide treatment.

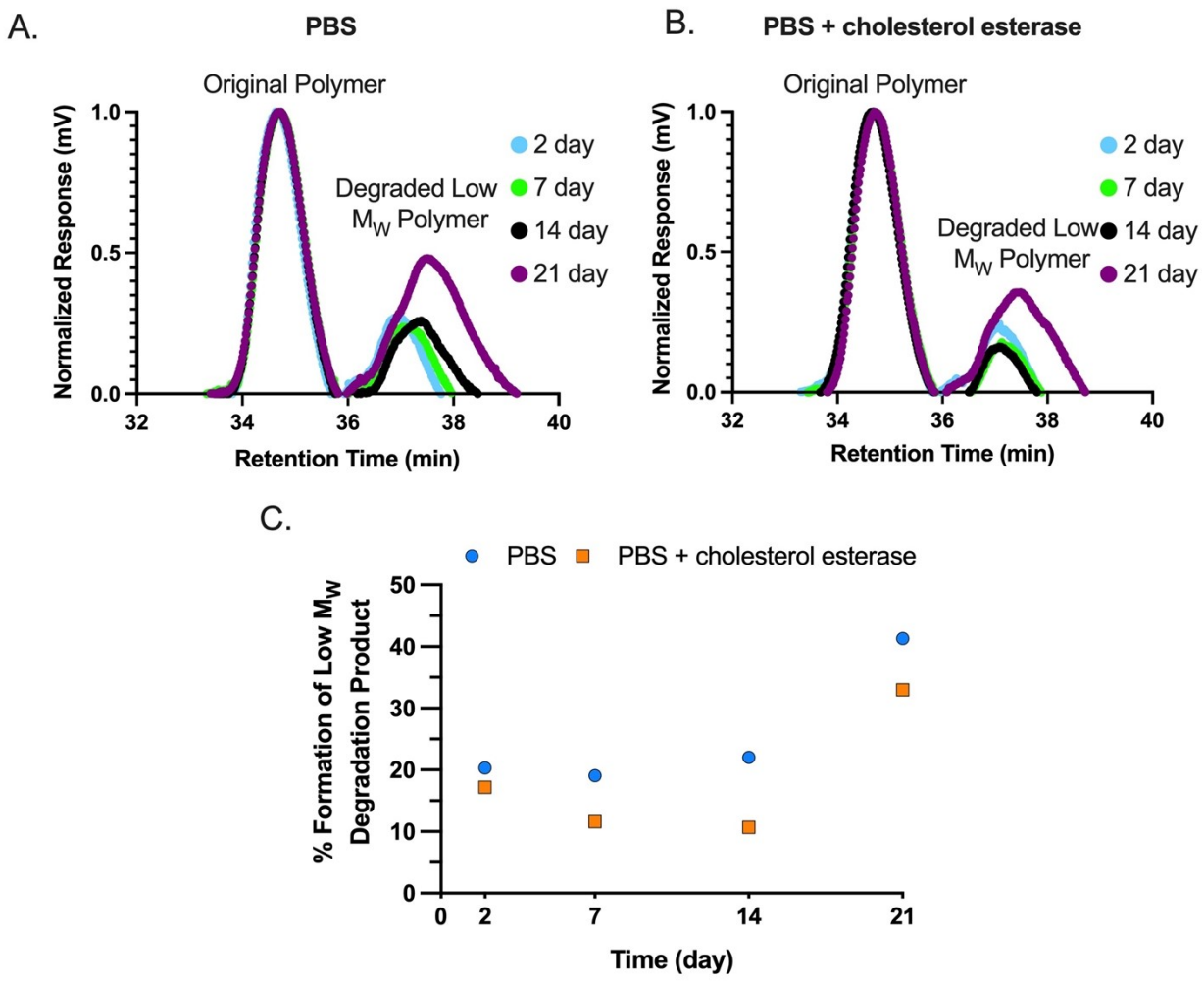

Figure S14. (GA-*co*-GB)-87 degradation monitored by GPC over the course of three weeks. **A**. GPC trace of degradation samples in PBS. **B.** GPC trace of degradation samples in PBS and cholesterol esterase. **C.** Percent formation of low molecular weight degradation product, calculated from the area change in each GPC trace.

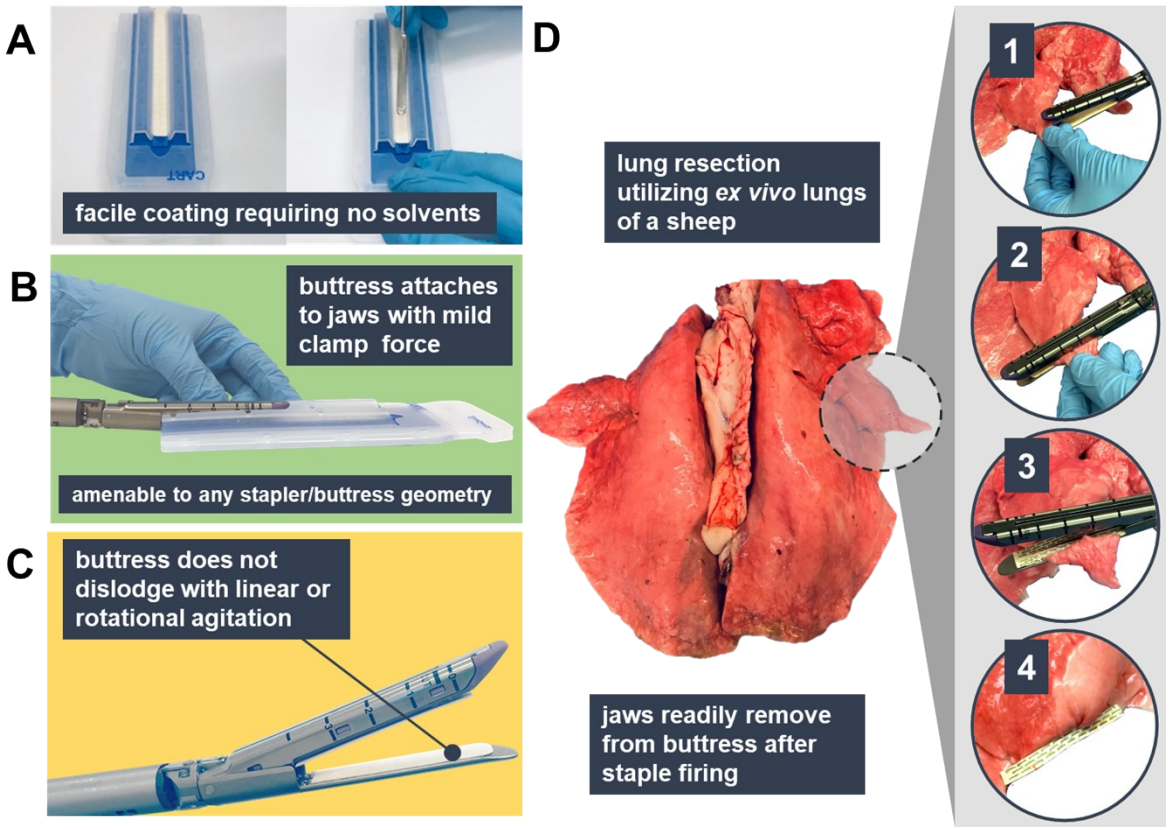

Figure S15. A. Coating of (GA-co-GB)-87 adhesive to bovine pericardium collagen buttress. **B** Attachment of the adhesive coated collagen buttress to the jaws of a surgical stapler and removal from the manufacture packaging. **C** Continual agitation, rotation, and closing/opening of the surgical stapler does not detach the buttress from the jaws. **D** Surgical resection of lung tissue using the adhesive coated collagen buttress attached to the jaws of a surgical stapler. After stapler firing, the buttress detaches from the jaws with jaw release and a slight pulling force requiring no additional maneuvers.

TABLES

f_{GA}	f_{GB}	F_{GA}	F_{GB}	% Conversion (W)	X	Y	ζ_1	ζ_2
10	90	13.17365	86.82635	0.72	0.111111	0.151724	0.95451	0.69901
30	70	32.57329	67.42671	0.82	0.428571	0.483092	0.895093	0.794075
50	50	51.02041	48.97959	0.67	1	1.041667	0.685179	0.657772
70	30	70.92199	29.07801	0.42	2.333333	2.439024	0.426417	0.407939
90	10	87.7193	12.2807	0.49	9	7.142857	0.475029	0.598537

Z	G	F	η	ξ	α	μ
2.573766	-0.32959	0.022904	-0.55324	0.038447	0.572835	1.241379
1.426791	-0.36229	0.237306	-0.44719	0.292919	0.572835	1.241379
1.077847	0.038657	0.896633	0.026307	0.610175	0.572835	1.241379
1.060493	1.356939	2.168705	0.494955	0.791054	0.572835	1.241379
0.706098	8.699727	14.32657	0.583897	0.961553	0.572835	1.241379

Table S1. Extended Kelen-Tudos plot of GA/GB/CO_2 terpolymerization.[4]

[f_{GA}] = mmol of glycidyl acetate monomer in feed. [f_{GB}] = mmol of glycidyl butyrate monomer in feed. [F_{GA}] = % of GA monomer incorporated into polymer chains. [F_{GB}] = % of GB monomer incorporate into polymer chains. $X = f_{GA}/f_{GB\ (Monomer\ feed)}$, $Y = F_{GA}/F_{GB\ (Polymer\ incorporation)}$, $\zeta_1 = \zeta_2(Y/X)$, $\zeta_2 = W(\mu+X)/(\mu+Y)$, $Z = log(1-\zeta_1)/log(1-\zeta_2)$, $G = (Y-1)/Z$, $F = Y/Z^2$ $\eta = (G)/(\alpha+F)$, $\xi = F/(\alpha+F)$, $\alpha = (F_{min}\, x\, F_{max})^{1/2}$, $\mu = M_2/M_1$.

Reference	Catalyst	Monomer	Selectivity of carbonate linkages
31	N,N'-[SalcyCo^{III}Cl]/PPNCl	propylene oxide	>99%
32	rac-[SalcyCo^{III}DNP]/DNP	derivatized oxiranes	>99%
33	Al^{Me}/PPNCl	limonene oxide	>99%
34	rac-/(S,S)-[SalcyCo^{III}DNP]	rac-(R)-benzyl glycidate	>99%
35	[LZnMg(C_6F_5)$_2$]	ε-decalactone; cyclohexene oxide	>99%
36	LInX	cyclohexene oxide	>99%
37	R,R-[SalcyCo^{III}DNP]	tert-butyl 3,4-epoxybutanoate	>99%
38	[(BDI)ZnOAc]	limonene oxide	N.R.
39	R,R-[SalcyCo^{III}Cl]/PPNCl	mPEG; 1,2-butylene oxide	N.R.
40	N,N'-[SalcyCo^{III}DNP]/PPNDNP	indene oxide	N.R.
41	N,N'-[SalcyCo^{III}OAc]	propylene oxide	>99%

Table S2. Organometallic catalysts used for the preparation for polycarbonates from epoxide monomers. N.R. = not reported.

REFERENCES

1. Araujo, Y.K.J., *et al*. Synthesis and enzymatic resolution of racemic 2,3-epoxy propyl esters obtained from glycerol. *Tetrahedron Letters* **2015**, 56, 1696–1698.

2. Lu, XB., *et al*. Highly active, bifunctional Co(III)-salen catalyst for alternating copolymerization of CO_2 with cyclohexene oxide and terpolymerization with aliphatic epoxides. *Macromolecules* **2010**, 43**,** 1396-1402**.**

3. Ren, W. M. *et al.* Mechanistic aspects of the copolymerization of CO_2 with epoxides using a thermally stable single-site cobalt(III) catalyst. *J. Am. Chem. Soc.* **2009,** 131**,** 11509–11518.

4. Kelen, T., Tüdos, F. A new improved linear graphical method for determining copolymerization reactivity ratios. *React. Kinet. Catal. Lett.* **1974**, 1, 487-492.